Structures 28 (2020) 2188–2202

Contents lists available at ScienceDirect

Structures

journal homepage: www.elsevier.com/locate/structures

Simultaneous sizing, shape, and layout optimization and automatic member grouping of dome structures

José P.G. Carvalho [a], Afonso C.C. Lemonge [b,*], Patrícia H. Hallak [b], Dênis E.C. Vargas [c]

[a] Postgraduate Program of Civil Engineering, Faculty of Engineering, Federal University of Juiz de Fora, Brazil
[b] Department of Applied and Computational Mechanics, Faculty of Engineering, Federal University of Juiz de Fora, Brazil
[c] Federal Institute of Education Science and Technology of Southeast of Minas Gerais – Campus Rio Pomba, Brazil

ARTICLE INFO

Keywords:
Large-scale structures
Sizing
Shape and layout optimization
Automatic member grouping
Frequency constraints
Stability constraints
Cardinality constraints
Differential evolution

ABSTRACT

This paper presents both discrete and continuous sizing, shape, and layout structural optimization problems concerning the weight minimization of dome structures and considering displacements, stresses, natural frequencies of vibration, and global stability as constraints. The layout optimization searches for the best structural configuration through the maintenance of the bars' grouping by introducing a new design variable. This variable refers to the number of standard modules used to generate the structural configuration of optimized domes. It can be attractive to use a reduced number of distinct cross-sectional areas, minimizing the costs of fabrication, transportation, storing, checking, and welding, providing labor saving measures. To obtain an automatic member grouping of the bars of the trusses analyzed in this paper, a specific encoding using cardinality constraints is considered. As result, trade-off curves are provided, showing the optimized weights in comparison with the number of distinct cross-sectional areas used in the solutions. Differential Evolution is the search algorithm adopted in this paper. The structural optimization problems showed better solutions when compared with those presented in the literature.

1. Introduction

In recent decades, metaheuristics have become attractive tools for solving optimization problems. In general, they have the advantage of not requiring the gradients of both functions to be optimized as well as their constraints. They handle discrete, continuous, mixed, and binary design variables well. In general, they are considered robust but may have the disadvantage of requiring an excessive number of objective function evaluations, especially when a simulator is needed to evaluate the objective function and/or constraints of the optimization problem when they are present in the formulation of the problem.

The sizing structural optimization of trusses and frames searches for the dimensions or the cross-sectional areas of the bars, for instance. Shape optimization searches for the best shapes of structures (e.g., finding the optimal coordinates of nodal points). On the other hand, topological optimization seeks the optimum structural configuration by maintaining or eliminating bars or groups of bars in the optimized solution. It is well-known that decreasing the member grouping will increase the weight of the structure. Finding the best member grouping is not a trivial task. To obtain automatic variable linking to search for the best member grouping of the bars of the trusses analyzed in this paper, a specific encoding involving cardinality constraints is considered. In this sense, apart from the sizing, shape, topological, and layout optimization, this paper also uses a strategy, previously presented by Barbosa and Lemonge [1] and Barbosa et al. [1] that enables the automatic grouping of bars.

Commonly, the constraints considered in the structural optimization problems do not include the natural frequencies of vibrations as well as the global stability regarding the critical buckling loads. For instance, buckling constraints are mostly checked at the bar level, evaluating the Euler elastic buckling load, rather than globally, and the natural frequencies of vibration are generally neglected. In addition to the usual constraints, such as nodal displacements and axial stresses, an optimized structure can be designed by making, at least, the first natural frequency of vibration high to avoid problems with resonance and the elastic critical loads concerning the global stability that can lead to the collapse of the structure or the discomfort of the users.

Differential evolution (DE), as proposed by Storn and Price [2], is

* Corresponding author.
E-mail addresses: jose.carvalho@engenharia.ufjf.br (J.P.G. Carvalho), afonso.lemonge@ufjf.edu.br (A.C.C. Lemonge), patricia.hallak@ufjf.edu.br (P.H. Hallak), denis.vargas@ifsudestemg.edu.br (D.E.C. Vargas).

https://doi.org/10.1016/j.istruc.2020.10.016
Received 21 April 2020; Received in revised form 7 October 2020; Accepted 8 October 2020
Available online 29 October 2020

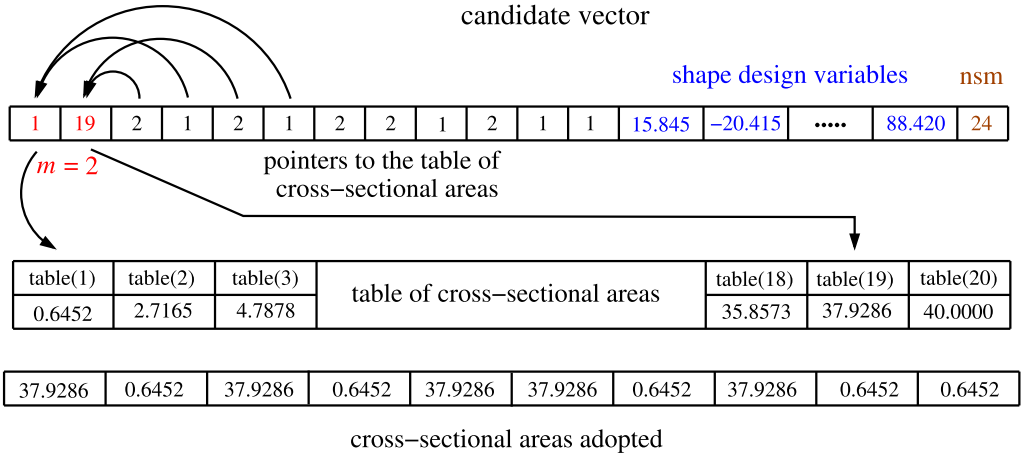

Fig. 1. Example of encoding for one vector with discrete sizing design variables. Shape and layout design variables are continuous and discrete, respectively.

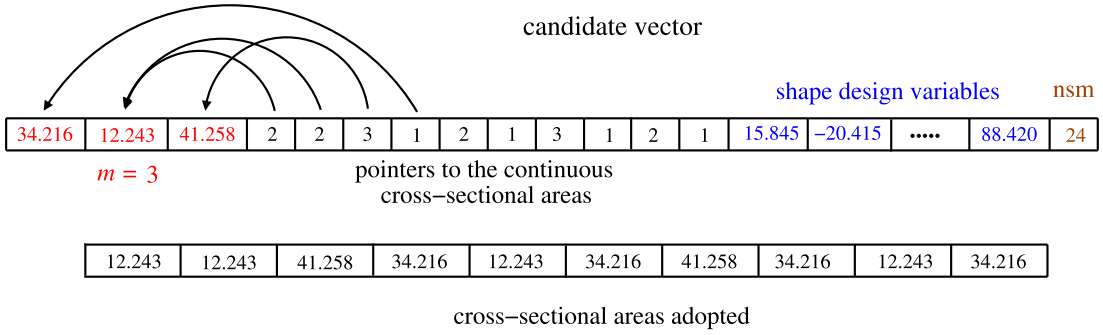

Fig. 2. Example of encoding for one vector with continuous sizing design variables. Shape and layout design variables are continuous and discrete, respectively.

used as the search algorithm, and the adaptive penalty method (APM), proposed by Barbosa and Lemonge [3,4], is the penalty scheme used to handle the constraints presented in the structural optimization problems discussed in this paper.

The objective of this paper is the application of DE and a strategy to automatically group the bars, to find optimized solutions considering sizing, shape, layout, and topology design variables simultaneously. The use of modules as design variables (in domes structures optimization problems), simultaneously with the sizing and topological design variables (also considering the possibility of grouping the bars), can be viewed as an innovative aspect proposed in this paper. Three numerical experiments are discussed: (i) a small-scale 120-bar single-layer truss dome; and two large-scale truss domes: (ii) a 600-bar single-layer truss dome and (iii) a 1410-bar double-layer truss dome. The structural optimization problems showed better solutions when compared with those presented in the literature.

The remainder of the paper is organized as follows. Section 2 presents some related works similar to those discussed in this paper. Section 3 describes the general formulation of the truss structural optimization problem. Section 4 describes the DE algorithm and the constraint-handling technique. Section 5 details the design variables and the special encoding for a candidate vector in DE. Section 6 presents the numerical experiments and the analysis of the results. Finally, the paper ends with conclusions and future work in Section 7.

2. Related work

In the literature, one can find multiple approaches regarding the topology optimization of trusses. Among these are gradient-based methods. For example, Bendsøe and Sigmund's book is an important reference [5]. One also recommends, among others, papers from Mela [6], Ramos and Paulino [7], and Kanno [8]. Furthermore, recent works in topology optimization have made possible the use of multi-materials with non-linear behavior analyses [9].

Pioneering studies using evolutionary algorithms coupled with a genetic algorithm for topology truss optimization have been reported since the 1990s, such as the works of Ohsaki [10], Hajela and Lee [11], Rajan [12], Tang et al. [13], Giger and Ermanni [14], Rahami et al. [15], Chen et al. [16], and Assimi et al. [17]. Metaheuristics were also applied in the topology optimization of trusses. The firefly algorithm was used by Fadel et al. [18] and Wu et al. [19]. Luh and Lin [20] and Mortazavi and Togan [21] applied a particle swarm optimization algorithm and its improvements. DE was the metaheuristic used in the works of Wu and Tseng [22], Huang and Xie [23], Zuo and Xie [24], Kitayama et al. [25], Ahrari et al. [26], Ho–Huu et al. [27], Kaveh and Mahdav [28], and Savsani et al. [29].

Automatic member grouping in structural optimization is desirable, but few papers in the literature present methods to solve this issue. An extended and commented review about this subject was presented by Carvalho et al. [30]. Some contributions in this field were presented by Biedermann and Cameron [31], Galante [32], Shea et al. [33], Barbosa and Lemonge [1], Barbosa et al. [34], Lemonge et al. [35], Barbosa and Lemonge [36], Kaveh and Zolgahdr [37], Herencia et al. [38], Guo and Li [39], Liu et al. [40], Liu et al. [41], Kripka et al. [42], Souza et al. [43], Tugilimana et al. [44], and Kaveh et al. [45].

Concerning the structural optimization of domes, such as that discussed in this paper, several works are presented in the literature. Saka and Ulker [46] developed a structural optimization algorithm for geometrically nonlinear three-dimensional trusses subject to displacement, stress, and cross-sectional area constraints. In [47], Ebenau et al. used an evolutionary strategy combined with an adaptive penalty function to solve shape and sizing linear and nonlinear structural

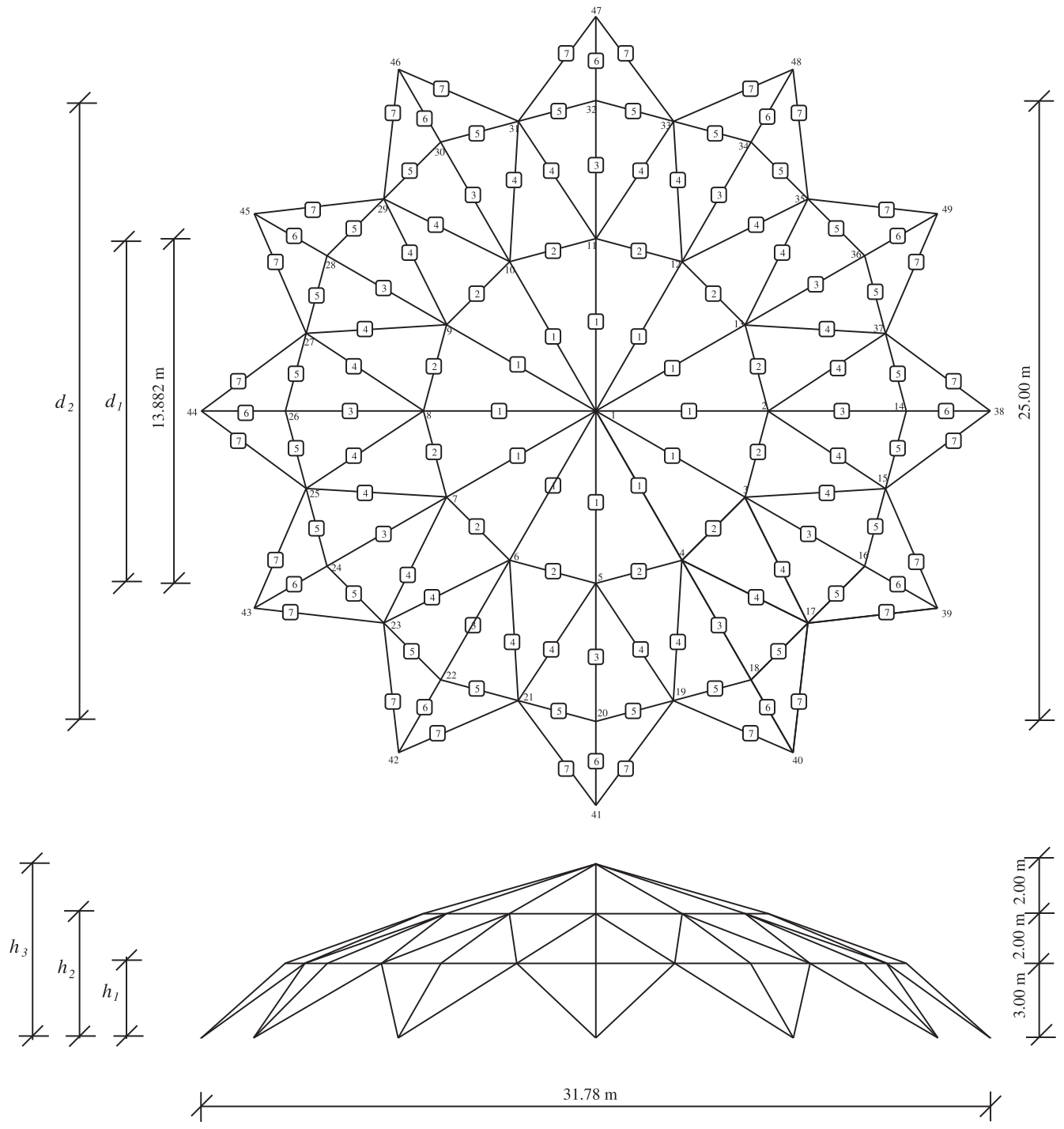

Fig. 3. The baseline 120-bar truss.

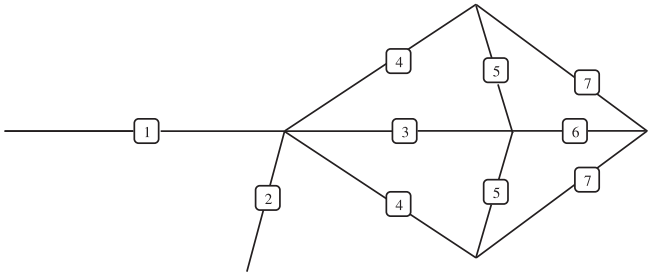

Fig. 4. The standard module and the original grouping of bars.

optimization problems under stress and displacements constraints. Saka [48] presented a study on the optimum topological design of geometrically nonlinear single-layer latticed domes using a genetic algorithm, considering buckling and displacements constraints.

Kameshki and Saka [49] adopted a genetic algorithm to find the optimum geometry design of nonlinear braced domes, under buckling and displacements constraints, considering the nonlinear response of the dome given the effect of axial forces on the flexural stiffnesses of members. A hybrid Big-Bang Crunch algorithm was presented by Kaveh and Talatahari [50] to find the optimum topology design of Schwedler and ribbed domes under buckling and displacements constraints. A comparative study concerning the optimum design of several types of

Table 1
Bounds of the design variables for the 120-bar truss dome.

Design variable	Bounds
sizing	2 cm^2 $\leqslant A_i \leqslant$ 140 cm^2
number std. modules	$8 \leqslant nsm \leqslant 16$
shape (height)	2.20 m $\leqslant h_1 \leqslant$ 2.70 m , 4.50 m $\leqslant h_2 \leqslant$ 5.50 m, 7.20 m $\leqslant h_3 \leqslant$ 7.50 m
shape (diameter)	13.50 m $\leqslant d_1 \leqslant$ 14.50 m, 24.50 m $\leqslant d_2 \leqslant$ 25.50 m

Table 2
The best results of the 120-bar truss dome, where areas A_i are given in cm^2 heights h_i and diameters d_i are given in meters. *nnp* and *nbar* are the number of nodes and number of bars of the dome, respectively. *nfe* is the number of function evaluations.

Case #	1	2	$3_{m=1}$	$3_{m=2}$	$3_{m=3}$	$3_{m=4}$
A_1	37.63	24.91	7.22	2.72	4.38	3.00
A_2	42.74	45.72	7.22	11.90	11.41	11.96
A_3	15.21	23.32	7.22	2.72	4.38	5.13
A_4	21.31	16.82	7.22	2.72	2.00	2.15
A_5	29.26	24.17	7.22	2.72	2.00	3.00
A_6	10.58	17.58	7.22	11.90	11.41	5.13
A_7	5.72	10.10	7.22	2.72	4.38	3.00
h_1	7.00	7.00	7.20	7.20	7.20	7.21
h_2	5.00	5.00	5.50	5.50	5.47	5.49
h_3	3.00	3.00	2.56	2.70	2.70	2.70
d_1	13.88	13.88	14.50	14.50	15.50	14.50
d_2	25.00	25.00	25.50	25.50	25.43	25.45
			Final dome configuration			
nsm	12	9	13	14	11	13
nnp	49	37	53	57	45	53
nbar	120	90	130	140	110	130
			Objective functions and constraints			
Weight (kg)	10310	8375	3780	2244	2122	1995
f_1 (Hz)	4.00	4.00	6.36	4.11	4.41	4.08
λ_{cr}	2.42	3.08	9.02	2.80	3.65	2.91
u_{max} (cm)	0.18	1.00	1.00	1.00	1.00	1.00
σ_{max} (MPa)	43.40	49.03	113.68	147.15	127.11	115.80
nfe	10000	10000	10000	10000	10000	10000

single-layer latticed domes was discussed by Kaveh and Talatahari [50].

The geometry and topology optimization of geodesic domes using a charged system search was given by Kaveh and Talatahari [51], consisting of finding optimal sections for elements, the optimal height for the crown, and the optimum number of elements (size, geometry, and topology optimization, respectively). The constraints concerned displacements, buckling, and shear stresses. Çarbaş and Saka [52] presented an optimum topological design algorithm to find the optimum number of rings, the optimum height of the crown, and optimum tubular section designations for the member groups of lattice domes. The harmony search algorithm was used, and buckling and displacements were the constraints. Babaei and Sheidaii [53] presented an algorithm to automate the optimal geometry and sizing design of the latticed space domes using parametric mathematical functions. The optimization problem was subjected to displacement, slenderness ratio, and stress constraints. Enhanced hybrid metaheuristic algorithms were proposed by Azad [54] for the optimal sizing of steel truss structures with numerous discrete variables, including domes structures. The optimization problems were subjected to displacements and buckling constraints. A design sensitivity analysis for the optimal design of geometrically nonlinear lattice structures considering limits for the nodal displacements, element stresses, and critical load factor, was presented by Fu et al. [55]. Chaos-based firefly algorithms for the sizing and shape optimization of cyclically large-sized braced steel domes with multiple frequency constraints were proposed by Kaveh and Javadi [56]. An interactive fuzzy search algorithm proposed by Mortazavi [57] was used in [58] to determine the size and layout optimization of truss structures with dynamic constraints.

The contribution of this paper, in comparison with several optimization methods and problems found in the works related here, is the consideration of a set of design variables simultaneously (i.e., shape, size, layout, and grouping of bars). None of these references formulated this structural optimization problem (e.g. the layout design variable and the grouping of bars made simultaneously). As a result, this paper can generate counter-intuitive optimized solutions in comparison with those presented in the literature.

The following section presents the general formulation of the structural optimization problem analyzed in this paper, with the definition of the objective function, the design variables, and the considered constraints as well as the equations that evaluate them. Section 4 describes the search algorithm used to find the best solutions to the structural optimization problem described in Section 3. Also, in this section, the constrained structural optimization problem is transformed into an unconstrained optimization problem considering a penalized objective function through a strategy for handling constraints. Section 5 shows how the design variables, for a given candidate solution, are grouped and how connections are made among them. Each of these variables is part of a candidate solution vector that participates in the optimization algorithm. This paper adopts the DE algorithm.

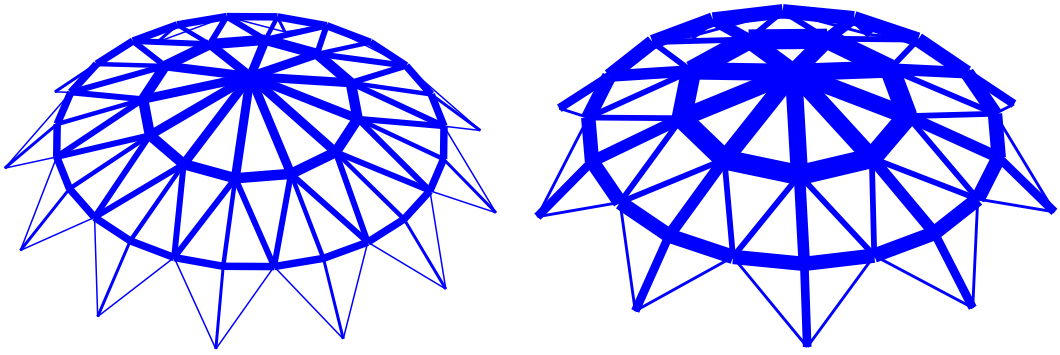

(a) Case #1 – 10310 kg (b) Case #2 – 8370 kg

Fig. 5. The best configurations of the 120-bar when cardinality constraints are not considered. The different thicknesses, not to scale, represent the different cross-sectional areas of each one of the bars.

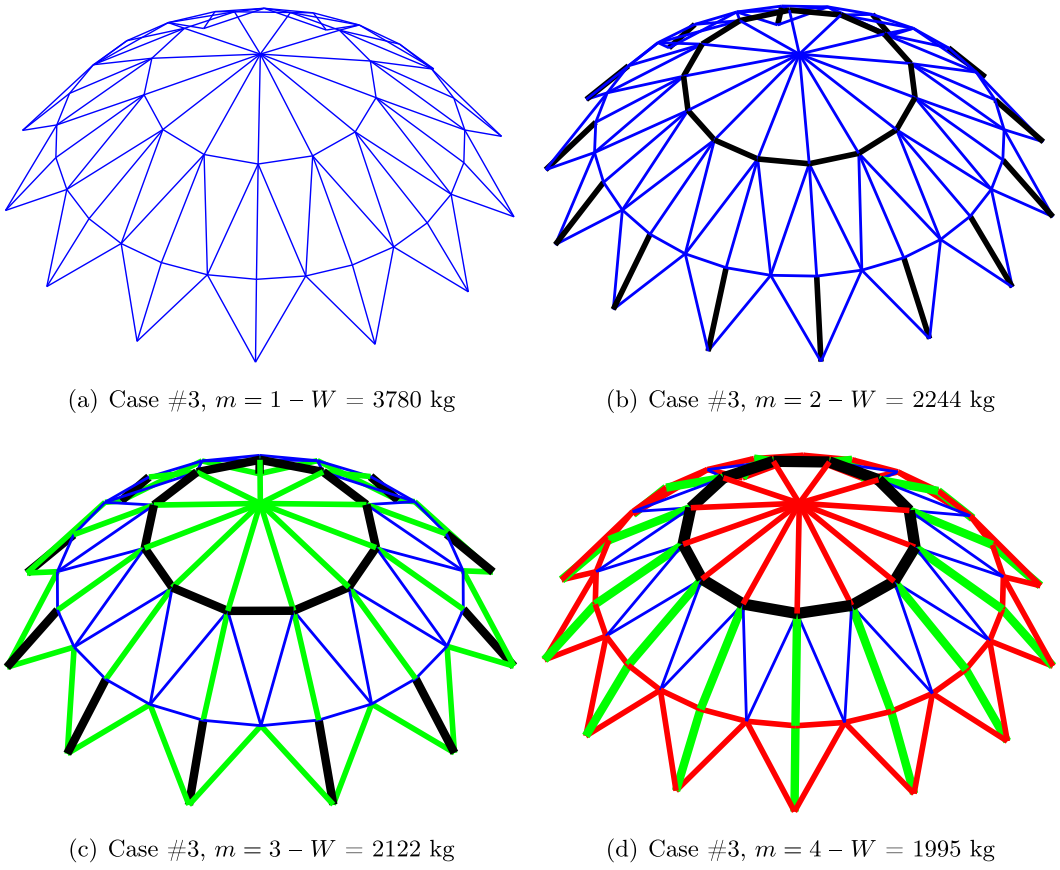

(a) Case #3, $m = 1 - W = 3780$ kg (b) Case #3, $m = 2 - W = 2244$ kg

(c) Case #3, $m = 3 - W = 2122$ kg (d) Case #3, $m = 4 - W = 1995$ kg

Fig. 6. The best configurations of the 120-bar truss dome when cardinality constraints are considered. The different colors indicate the different cross-sectional areas adopted in each group in the optimized solutions. (For interpretation of the references to color in this figure legend, the reader is referred to the web version of this article.)

3. General formulation of truss structural optimization problem

The problems analyzed in this paper refer to the sizing, shape, topology, and layout optimization of truss structures. The design variables are the cross-sectional areas of the bars (discrete or continuous – sizing), the presence or absence of a specific bar (topology), and the node coordinates (continuous – shape). The general formulation of the optimization problem presented in this section encompasses all the experiments presented in this paper. The objective function is the same for each of them, and the problems differ only in the set of design variables and constraints. The objective function is the weight $W(\mathbf{x})$ of the structure to be minimized and written as:

$$W(\mathbf{x}) = \sum_{i=1}^{N} \rho A_i L_i, \tag{1}$$

where ρ is the specific mass of the material and A_i and L_i are the cross-sectional areas and the length of the i-th bar of the structure, respectively. The number of bars of the structure is denoted by N.

The design variables are $\mathbf{x} = \{A_1, A_2, \ldots, A_N, X_i, Y_i, Z_i, nsm\}$, where A_i are the sizing design variables indicating the cross-sectional areas of the bars (continuous or discrete), X_i, Y_i, Z_i are the shape design variables (continuous), and finally, nsm is a layout design variable (discrete) that is defined later in this text. The search space of the design variables is defined by the lower $\mathbf{x}^L$ and upper $\mathbf{x}^U$ bounds, respectively.

In the problem formulations, the constraints are normalized, such as:

$$\frac{u_j(\mathbf{x})}{\overline{u}} - 1 \leqslant 0, \quad 1 \leqslant j \leqslant m_u, \tag{2}$$

$$\frac{\sigma_i(\mathbf{x})}{\overline{\sigma}} - 1 \leqslant 0, \quad 1 \leqslant i \leqslant m_\sigma, \tag{3}$$

$$1 - \frac{f_l(\mathbf{x})}{\overline{f}} \leqslant 0, \quad 1 \leqslant l \leqslant m_f, \tag{4}$$

$$1 - \frac{\lambda_l(\mathbf{x})}{\overline{\lambda}} \leqslant 0, \quad 1 \leqslant l \leqslant m_\lambda, \tag{5}$$

where m_u is the degree of freedom of the structure, $m_\sigma = N$ is the total

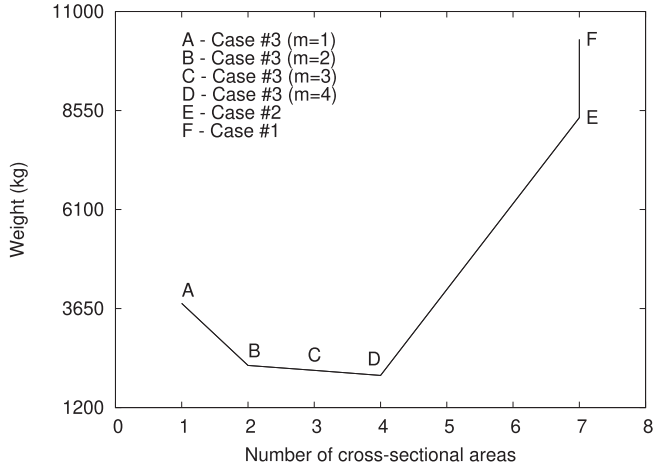

Fig. 7. The trade-off between weight and number of different cross-sectional areas for the 120-bar single-layer truss dome.

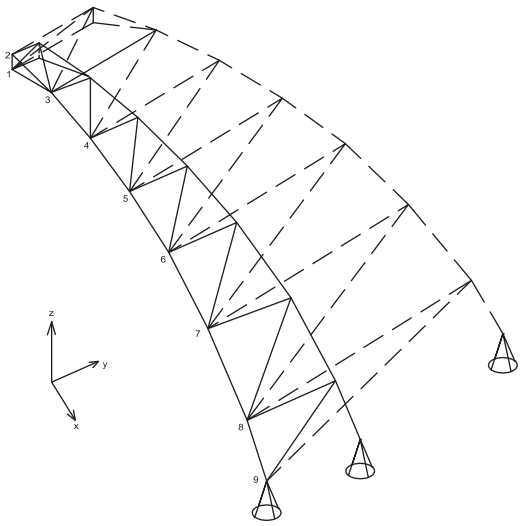

	Coordinates		
Node	x	y	z
1	1.00	0.00	7.00
2	1.00	0.00	7.50
3	3.00	0.00	7.25
4	5.00	0.00	6.75
5	7.00	0.00	6.00
6	9.00	0.00	5.00
7	11.00	0.00	3.50
8	13.00	0.00	1.50
9	14.00	0.00	0.00

Fig. 8. Standard module for 600-bar single-layer truss, with two possible meshes according to the number of modules.

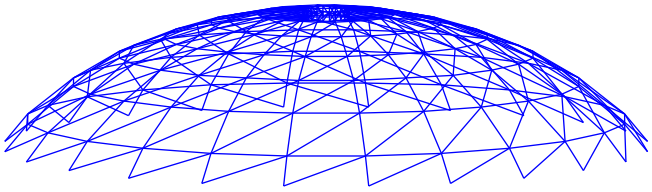

Fig. 9. 600-bar single-layer truss dome with 30 standard modules – 3D view.

number of bars, m_f is the total number of constrained natural frequencies of vibration, and m_λ is the total number of constrained load factors of the structure. The allowable displacements, stresses, natural frequency of vibration, and load factor are defined by $\overline{u}, \overline{\sigma}, \overline{f}$, and $\overline{\lambda}$, respectively.

The nodal displacements $\{u\}$ are obtained by the equilibrium equation for a discrete system of bars, which is written as:

$$[K]\{u\} = \{p\}, \tag{6}$$

where $[K]$ is the stiffness matrix and $\{p\}$ are the load components [59].

The natural frequencies of vibration are obtained by the evaluation of the eigenvalues of the matrix

$$\left([K] - f_{m_f}^2[M]\right)\phi_{m_f} = 0, \tag{7}$$

where $[M]$ is the mass matrix and ϕ_{m_f} is the m_f-th eigenvector corresponding to the m_f-th eigenvalue [59].

The load factors λ concerning the global stability are obtained by the evaluation of the eigenvalues of the matrix

$$([K] + \lambda_{m_\lambda}[K_G])\nu_{m_\lambda} = 0, \tag{8}$$

where $[K_G]$ is the geometric matrix of the structure and λ_{m_λ} are the equivalent eigenvalues with respect to the m_λ load factors of the structure. The lowest value λ_{cr} of λ_{m_λ} gives the buckling load factor or critical load factor for the structure. The eigenvector ν_{m_λ} represents the corresponding deformation of the structure [60].

4. The differential evolution algorithm and the constraint-handling technique

The optimization algorithm used to solve the constrained optimization problems presented in this paper is a third evolution step differential evolution (GDE3) algorithm, which is a modified version of the traditional DE algorithm proposed by Kukkonen and Lampinen [61], to improve the DE behavior. The DE algorithm adopted in this paper as the search machine was previously used to solve multi-objective structural optimization and showed excellent performance in [62].

Storn and Price [2] originally introduced the DE. The evolution of a population inspired the algorithm, which consisted of vectors in the search space; at each step, new vectors are generated by adding to a base vector a scaled difference between two other randomly chosen vectors of the previous generation as shown bellow, according to Price et al. [63].

An initial population is generated randomly and improved using DE's selection, mutation, and crossover operations, where the crossover rate ($CR \in [0,1]$), the mutation factor ($F \in \mathbb{R}$), and the population size (NP) are the parameters set by the user. The crossover and mutation operations are explained in Algorithm 1.

Let P_G be a population of NP decision vectors $\mathbf{x}_{i,G}$ in generation G, where $i \in \{1,2,3,\ldots,ndv\}$ is a vector index, where ndv is the number of design variables. Each $\mathbf{x}_{i,G}$ of the population in generation G is an n-dimensional vector, and $\mathbf{x}_{j,i,G}$ is its j-th component ($j \in \{1,2,3,\ldots,n\}$).

As presented in Algorithm 1, a decision vector $\mathbf{x}_{i,G}$ creates the corresponding trial vector $\mathbf{u}_{i,G}$ through mutation and crossover operations. As can be observed in this algorithm, three vectors $-\mathbf{x}_{r_1,G}, \mathbf{x}_{r_2,G}$ and $\mathbf{x}_{r_3,G}-$ are randomly selected in the population; they are mutually different and different from $\mathbf{x}_{i,G}$.

Algorithm 1 Mutation and Crossover DE Operations.

1: Select randomly $J \in \{1,\ldots,n\}$
2: **for** $j = 1 : n$ **do**
3: Select randomly $rand \in [0,1]$
4: **if** $rand < CR$ or $j = J$ **then**
5: $\mathbf{u}_{j,i,G} \leftarrow \mathbf{x}_{j,r_1,G} + F(\mathbf{x}_{j,r_2,G} - \mathbf{x}_{j,r_3,G})$
6: **else**
7: $\mathbf{u}_{j,i,G} \leftarrow \mathbf{x}_{j,r_1,G}$
8: **end if**
9: **end for**

Table 3
Results for the 600-bar single-layer truss dome, where areas A_i are in cm^2, *nnp* and *nbar* are the number of nodes and number of bars of the complete module, respectively.

Case #	1	[68]	[30]	[56]	2	$3_{m=1}$	$3_{m=2}$	$3_{m=3}$	$3_{m=4}$
A_1	1.00	1.0299	1.50	1.3190	1.00	8.00	4.00	7.00	3.00
A_2	1.50	1.3664	1.50	1.3826	1.50	8.00	4.00	7.00	7.50
A_3	6.50	5.1095	7.00	4.9379	1.00	8.00	4.00	7.00	9.00
A_4	5.50	1.3011	1.00	1.3222	3.50	8.00	4.00	4.50	3.00
A_5	17.00	17.0572	16.50	17.1285	20.00	8.00	12.00	14.00	9.00
A_6	41.00	34.0764	34.50	37.4657	34.00	8.00	12.00	14.00	10.00
A_7	12.00	13.0985	12.00	12.7071	12.00	8.00	12.00	14.00	10.00
A_8	17.00	15.5882	15.50	15.4252	25.00	8.00	12.00	7.00	7.50
A_9	11.00	12.6889	10.50	11.3642	28.00	8.00	4.00	7.00	7.50
A_{10}	9.50	10.3314	10.00	9.3343	16.00	8.00	4.00	7.00	7.50
A_{11}	9.00	8.5313	8.50	8.3872	3.50	8.00	4.00	4.50	9.00
A_{12}	8.50	9.8308	9.00	9.1101	7.50	8.00	12.00	7.00	9.00
A_{13}	7.50	7.0101	7.50	7.1472	8.00	8.00	12.00	4.50	9.00
A_{14}	4.50	5.2917	5.50	5.1701	3.00	8.00	4.00	4.50	3.00
A_{15}	6.00	6.2750	6.50	6.6239	5.00	8.00	12.00	4.50	7.50
A_{16}	5.00	5.4305	5.50	5.2427	4.50	8.00	4.00	14.00	9.00
A_{17}	4.00	3.6414	5.00	3.5213	3.50	8.00	4.00	4.50	3.00
A_{18}	8.00	7.2827	7.50	7.6096	5.50	8.00	12.00	7.00	9.00
A_{19}	4.50	4.4912	4.50	4.2877	10.00	8.00	12.00	4.50	9.00
A_{20}	2.00	1.9275	2.00	2.1684	2.00	8.00	4.00	4.50	3.00
A_{21}	4.50	4.6958	4.50	4.6704	3.50	8.00	4.00	4.50	7.50
A_{22}	4.50	3.3595	4.00	3.5380	4.50	8.00	4.00	7.00	7.50
A_{23}	2.50	1.7067	2.00	1.8252	5.50	8.00	4.00	4.50	3.00
A_{24}	5.00	4.8372	4.50	4.8110	4.00	8.00	4.00	4.50	3.00
A_{25}	1.50	2.0253	1.50	1.6589	1.50	8.00	4.00	4.50	3.00
					Final dome configuration				
nsm	24	24	24	24	19	18	18	18	18
nnp	216	216	216	216	171	162	162	162	162
nbar	600	600	600	600	475	450	450	450	450
					Objective functions and constraints				
W (kg)	6196	6175	6132	6058.49	5957	6947	5776	5360	5282
f_1 (Hz)	5.0616	5.0013	5.0231	5.00	5.0343	6.7614	5.8062	5.8979	5.5887
f_3 (Hz)	7.0010	7.0049	7.0013	7.00	7.0069	7.0655	7.0205	7.0037	7.0006
nfe	32000	20000	20000	10000	16000	6000	9000	12000	15000

Considering both the trial vector $\mathbf{u}_{i,G}$ and the decision vector $\mathbf{x}_{i,G}$ feasible, the trial vector $\mathbf{u}_{i,G}$ is selected to replace the decision vector $\mathbf{x}_{i,G}$ in the next generation P_{G+1} (population in generation $G+1$) if $f(\mathbf{u}_{i,G}) < f(\mathbf{x}_{i,G})$, where f is the objective function. Otherwise, $\mathbf{u}_{i,G}$ is discarded, and $\mathbf{x}_{i,G}$ remains in the population.

To handle the constraints, the APM proposed by Barbosa and Lemonge [3,4] is adopted here to enforce all the mechanical constraints considered in the numerical experiments. The constrained optimization problem is transformed into an unconstrained optimization problem by introducing a penalty function in Eq. (1). Consider the fitness function

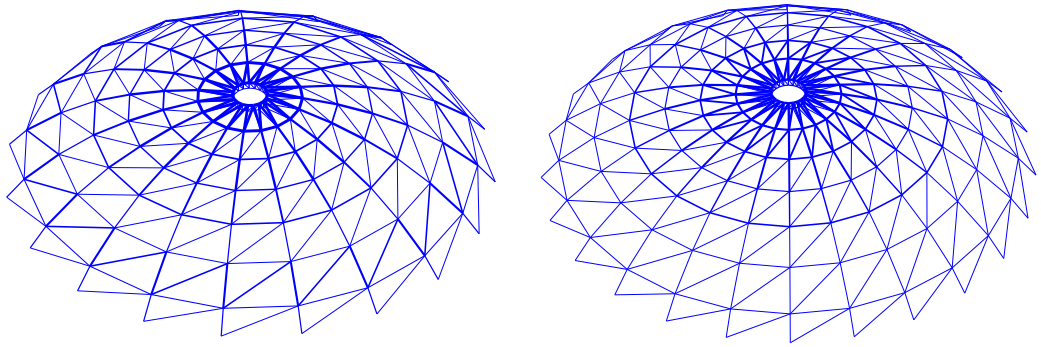

(a) Case #1 – $W = 6196$ kg (b) Case #2 – $W = 5957$ kg

Fig. 10. The best configurations of the 600-bar when cardinality constraints are not considered. The different thicknesses, not to scale, represent the different cross-sectional areas of each one of the bars.

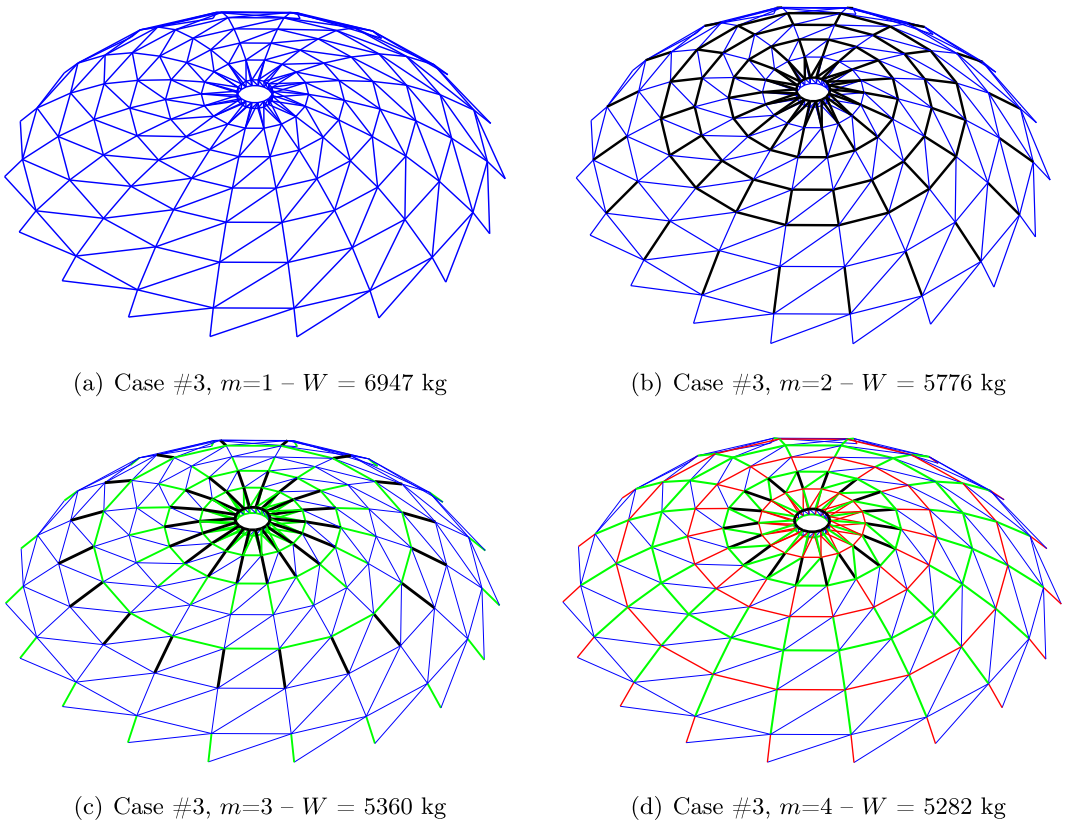

(a) Case #3, m=1 – W = 6947 kg (b) Case #3, m=2 – W = 5776 kg

(c) Case #3, m=3 – W = 5360 kg (d) Case #3, m=4 – W = 5282 kg

Fig. 11. The best configurations of the 600-bar truss dome when cardinality constraints are considered. The different colors indicate the different cross-sectional areas adopted in each group in the optimized solutions.

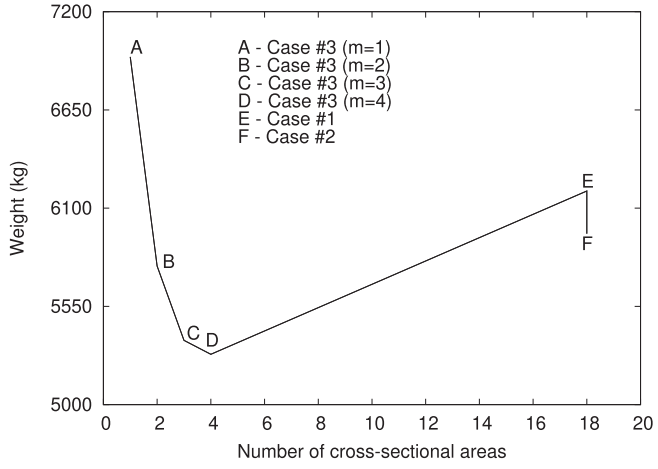

Fig. 12. The trade-off between weight and number of different cross-sectional areas for the 600-bar single-layer truss dome.

$F(\mathbf{x})$) (penalized or not) of the problem without constraints and $f(\mathbf{x})$ the objective function. To facilitate the description of the APM, $f(\mathbf{x})$ is the objective function and the same function as that in Eq. (1) (i.e., $f(\mathbf{x}) = W(\mathbf{x})$), and the fitness function is written as:

$$F(\mathbf{x}) = \begin{cases} f(\mathbf{x}), & \text{if} \quad \mathbf{x} \quad \text{is feasible} \\ \bar{f}(\mathbf{x}) + \sum_{jj=1}^{n_c} k_{jj} v_{jj}(\mathbf{x}), & \text{otherwise} \end{cases} \tag{9}$$

where $F(\mathbf{x})$ is the weight of the structure with no penalization (Eq. 1), and

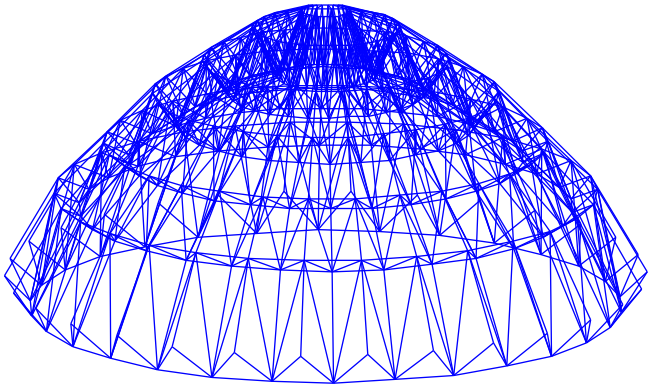

Fig. 13. Standard 1410-bar double-layer truss dome proposed by Kaveh et al. [68] with 30 standard modules.

$$\bar{f}(\mathbf{x}) = \begin{cases} f(\mathbf{x}), & \text{if} \quad f(\mathbf{x}) > \langle f(\mathbf{x}) \rangle \\ \langle f(\mathbf{x}) \rangle, & \text{if} \quad f(\mathbf{x}) \leqslant \langle f(\mathbf{x}) \rangle \end{cases} \tag{10}$$

where $\langle f(\mathbf{x}) \rangle$ is the average value of the objective function of the current population. The penalty parameter k_{jj} is defined as

$$k_{jj} = |\langle w(\mathbf{x}) \rangle| \frac{\langle v_{jj}(\mathbf{x}) \rangle}{\sum_{ll=1}^{n_c} [\langle v_{ll}(\mathbf{x}) \rangle]^2}, \tag{11}$$

where $\langle v_{jj}(\mathbf{x}) \rangle$ means the violation of the *jj-th* constraint (see Eqs. (2)–(5)) averaged over the current population considering only infeasible individuals.

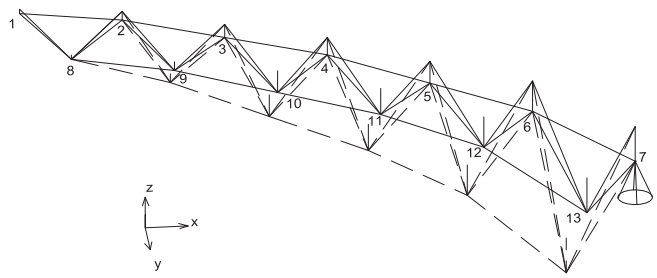

	Coordinates		
Node	x	y	z
1	1.00	0.00	4.00
2	3.00	0.00	3.75
3	5.00	0.00	3.25
4	7.00	0.00	2.75
5	9.00	0.00	2.00
6	11.00	0.00	1.25
7	13.00	0.00	0.00
8	1.989	0.209	3.00
9	3.978	0.418	2.75
10	5.967	0.627	2.25
11	7.956	0.836	1.75
12	9.645	1.045	1.00
13	11.934	1.254	-0.50

Fig. 14. Standard module for 1410-bar single-layer truss, with two possible meshes according to the number of modules.

5. Design variables and special encoding for a candidate vector in DE

As defined in Section 3, the design variables are the cross-sectional areas of the bars (continuous or discrete), the shape design variables (continuous), and the layout design variable (discrete). The domes discussed in this paper are submitted to weight minimization, and all of them are made up of standard modules that generate their whole structural configuration. The number of standard modules, denoted by *nsm*, is the new layout design variable to be considered in the formulation of the structural optimization problem.

In general, the number of sizing design variables results in a different value for each of them in the optimized solution. Of course, some of them may have the same value. Aspects concerning the symmetry of the structure are also mandatory in the definition of groupings of the sizing design variables. Furthermore, to explore desirable advantages during the design configurations, a designer may require that, at most, a given m of distinct cross-sectional areas should be used in the final structural configuration, thus grouping the bar into m groups.

A special encoding to link the bars automatically was proposed by Barbosa and Lemonge [3] and extended to several applications, such as in Barbosa and Lemonge [1], Lemonge et al. [34], Barbosa and Lemonge [36], Carvalho et al. [30], and Kripka et al. [64,42].

Hence, the optimization problem must consider additional constraints requiring that no more than m ($m \leqslant N$) different cross-sectional areas should be used:

$$A_i \in C_m = \{S_1, S_2, \ldots, S_m\}, \quad i = 1, 2, \ldots, N,$$

where the cross-sectional areas $S_c, c = 1, 2, \ldots, m$ are unknown but belong to a larger area ($N > m$). These additional constraints can be defined as cardinality constraints, and $m = N$ means the standard structural optimization problem.

As an example of the encoding used in the experiments –including cardinality constraints to find the best member groupings, proposed by Barbosa and Lemonge in [1]– Figs. 1 and 2 illustrate two candidate vectors. The cardinality constraints, such as $m = 3$, shown in Fig. 2, are represented by the three continuous design variables at the left part of the encoding. Hence, the first m (m being the number of cardinality constraints) values of the vectors will lead to the cross-sectional areas chosen by the vector (they can discretely point to any value in a predefined table (Fig. 1) or be continuous (Fig. 2). The next n values correspond to the n cross-sectional areas of the structure. Finally, at the end of the vector, there are shape and layout (*nsm*), as well as design variables, respectively.

It is important to mention that the variables are considered continuous in the vector for better and appropriate DE behavior, and to obtain the correspondent discrete value, a rounded value is recovered. For example, if the continuous value is 1.431, then it will be rounded assuming an area 1 of the m possibilities. If in the new generation, this value changes to 1.588, it will be rounded to point to the area 2.

6. Numerical experiments

In this section, three numerical experiments are discussed: (i) a small-scale 120-bar single-layer truss dome; and two large-scale truss domes: (ii) a 600-bar single-layer truss dome and (iii) a 1410-bar double-layer truss dome. The experiments were performed in 20 independent runs, with the scale factor F equal to 0.4 and the crossover probability CR equal to 0.9. These values were indicated by Storn and Price [2]. A sensitivity analysis of these parameters was discussed by Krempser et al. [65].

6.1. A 120-bar single-layer truss dome

The dome depicted in Fig. 3 is a 120-bar three-dimensional truss previously discussed in the literature by Saka and Ulker [66], Ebenau et al. [67], and Lemonge et al. [35], among others. This dome is the baseline structure of the first numerical experiment. The dome is subjected to a downward vertical equal to 60 kN at node 1 (elevation h_3), 30 kN at nodes 2 to 13 (leading to a resulting load of 360 kN at this elevation h_2), and 20 kN at nodes 14 to 37 (leading to a resulting load of 240 kN at this elevation h_1). When *nsm* is a design variable, these respective resultants at each elevation are divided by the number of respective nodes according to *nsm*. The displacements are limited to 1 cm in the x,y, and z directions. The specific mass of the material is 7860 kg/m^3, Young's modulus is equal to 210 GPa, and the yielding stress is $\sigma_y = 240$ N/mm^2. The boundaries of cross-sectional areas are 2 cm^2 and 140 cm^2, respectively, the first natural frequency should be $f_1 \geqslant 4$ Hz, the number of standard modules must be in the range $8 \leqslant nsm \leqslant 16$, and the load factor concerning the global stability must be greater than or equal to 1.

Note that the dome is made up of standard modules, as depicted in Fig. 4, containing ten members grouped in seven distinct cross-sections. Thus, the dome shown in Fig. 3 presents 12 standard modules, leading to a total of 120 bars.

Three cases (#1, #2, and #3) are analyzed in this experiment, where *ndv* means the number of design variables in the following descriptions:

- In Case #1, only the sizing design variables (cross-sectional areas of the bars) are set ($ndv = 7$).
- In Case #2, a layout design variable (number of standard modules or *nsm*) is added ($ndv = 8$).
- Case #3 considers sizing (cross-sectional areas of the bars), shapes h_1, h_2, and h_3 (heights), diameters d_1 and d_2 (diameters), and layout design variables (number of standard modules or *nsm*), and a cardinality constraint m setting the maximum number of distinct cross-sectional areas of the bars ($ndv = 13 + m$).

The bounds for the design variables are defined in Table 1.
Table 2 shows the results for Cases #1 to #3 of the 120-bar truss

Table 4
Results for the 1410-bar double-layer truss dome, where areas A_i are in cm^2, *nnp* and *nbar* are the number of nodes and number of bars of the complete module, respectively.

Case #	1	[68]	[30]	[56]	2	$3_{m=1}$	$3_{m=2}$	$3_{m=3}$	$3_{m=4}$
A_1	3.50	7.9969	2.50	5.149	10.00	11.00	14.00	11.00	5.00
A_2	6.00	6.1723	6.00	4.406	2.50	11.00	3.50	3.50	2.50
A_3	26.00	35.5011	18.00	24.590	31.00	11.00	14.00	11.00	12.00
A_4	9.00	10.2510	9.50	9.166	11.00	11.00	14.00	11.00	12.00
A_5	6.00	5.3727	6.00	5.800	1.50	11.00	3.50	3.50	5.00
A_6	2.00	1.3488	1.00	1.883	3.50	11.00	3.50	3.50	5.00
A_7	27.00	11.4427	29.50	21.073	21.00	11.00	14.00	11.00	12.00
A_8	8.50	9.7157	8.00	8.739	9.50	11.00	14.00	11.00	9.50
A_9	1.50	1.3005	2.00	2.005	3.00	11.00	3.50	3.50	5.00
A_{10}	1.50	2.5046	1.50	2.398	30.00	11.00	3.50	3.50	5.00
A_{11}	1.50	10.7849	1.00	7.655	4.00	11.00	3.50	11.00	12.00
A_{12}	8.00	10.1954	7.50	9.971	17.00	11.00	14.00	11.00	9.50
A_{13}	1.50	2.2300	1.00	2.350	2.50	11.00	14.00	3.50	2.50
A_{14}	5.50	5.1186	6.00	5.024	2.00	11.00	3.50	4.50	2.50
A_{15}	15.00	14.0053	14.50	18.234	3.00	11.00	14.00	11.00	9.50
A_{16}	8.00	8.9713	9.00	8.825	5.50	11.00	14.00	11.00	9.50
A_{17}	2.50	4.0756	1.00	3.763	2.00	11.00	14.00	4.50	5.00
A_{18}	8.50	5.9211	8.00	5.723	3.50	11.00	14.00	4.50	5.00
A_{19}	16.00	10.6915	19.50	10.207	27.00	11.00	3.50	4.50	5.00
A_{20}	15.00	10.6220	16.50	13.046	12.00	11.00	14.00	11.00	12.00
A_{21}	4.50	4.5064	5.00	5.118	4.00	11.00	14.00	3.50	5.00
A_{22}	8.00	8.4086	9.00	7.340	4.50	11.00	3.50	4.50	5.00
A_{23}	1.00	5.8405	1.00	1.029	1.00	11.00	3.50	3.50	2.50
A_{24}	6.00	5.0342	5.00	4.479	2.00	11.00	3.50	3.50	5.00
A_{25}	3.50	3.8932	6.50	2.962	2.00	11.00	3.50	3.50	2.50
A_{26}	5.00	6.1647	5.00	4.519	5.50	11.00	3.50	3.50	5.00
A_{27}	7.00	6.8990	7.00	5.847	4.50	11.00	3.50	3.50	5.00
A_{28}	16.00	11.6387	15.50	11.750	4.00	11.00	3.50	11.00	5.00
A_{29}	4.50	3.8343	4.50	3.925	4.50	11.00	3.50	3.50	2.50
A_{30}	2.00	1.4772	2.50	1.697	2.50	11.00	3.50	4.50	5.00
A_{31}	1.50	1.3075	2.50	1.811	3.00	11.00	14.00	4.50	5.00
A_{32}	3.00	4.4876	1.00	3.698	8.00	11.00	14.00	3.50	2.50
A_{33}	5.50	6.0196	6.00	5.396	6.50	11.00	3.50	11.00	9.50
A_{34}	1.50	2.6729	1.00	2.392	2.00	11.00	3.50	3.50	5.00
A_{35}	1.50	1.6342	1.00	2.203	2.00	11.00	3.50	3.50	2.50
A_{36}	1.00	1.8410	1.00	2.718	1.50	11.00	3.50	3.50	2.50
A_{37}	11.00	6.8841	10.00	7.498	4.50	11.00	14.00	11.00	9.50
A_{38}	5.00	4.1393	5.50	4.840	4.50	11.00	14.00	11.00	5.00
A_{39}	3.00	3.3264	3.50	3.457	3.00	11.00	3.50	3.50	5.00
A_{40}	1.00	1.0000	1.00	1.005	1.00	11.00	3.50	4.50	5.00
A_{41}	7.50	6.9376	7.50	6.440	13.00	11.00	3.50	11.00	12.00
A_{42}	8.00	4.4568	8.50	5.787	9.50	11.00	3.50	3.50	5.00

dome. Fig. 5 shows the best configurations for the 120-bar when cardinality constraints are not considered (Cases #1 and #2). The different thicknesses, not to scale, represent the different cross-sectional areas of each bar. Fig. 6 shows the best configurations for the 120-bar truss dome when the cardinality constraints are considered (Case #3). The different colors indicate the different cross-sectional areas adopted in each group in the optimized solutions.

The optimized solution presented a final weight equal to 1995 kg against 10310 kg achieved by the worst optimized solution concerning the original configuration of this dome with only the sizing design variables (Case #1). When the layout design variable was added (Case #2), the best solution had a final weight equal to 8375 kg, decreasing by 18.77% in comparison with 10310 kg (Case #1).

On the other hand, a significant decrease in the weights of the optimized structures can be observed when all the design variables are considered (Case #3). The weights decrease as the value of m increases, as expected. The worst solution (Case #3, m = 1) presented a final weight equal to 3780 kg, better than that presented by Case #1 by 63.33%. In addition, this solution grouped the bars in equal cross-sectional areas, different from Cases #1 and #2, where it is possible to have seven different areas for the bars. The best solution added one standard module, four nodes, and ten bars to the original configuration of the 120-bar truss dome. Despite these additions, this solution (Case #3) showed a decrease of 80.65% compared to the solution of Case #1. It is important to remark that all the constraints are satisfied and that the optimized solutions are rigorously feasible. In five results, the constraint concerning the maximum displacement is active, while in two, the constraint concerning the first natural frequency of vibration is active. Fig. 6.1 depicts the trade-off between the weights and the numbers of different cross-sectional areas for the 120-bar truss dome for all cases. Note that the weights decrease as the number of distinct cross-sectional areas increases, as expected. The trade-off curves also show that the consideration of layout design variables and the optimal grouping of the bars significantly improve the results compared to the cases where only

Table 5
Results for the 1410-bar double-layer truss dome, where areas A_i are in cm^2 (continuation of Table 4).

Case #	1	[68]	[30]	[56]	2	$3_{m=1}$	$3_{m=2}$	$3_{m=3}$	$3_{m=4}$
A_{43}	6.00	4.6758	7.50	5.318	5.50	11.00	3.50	4.50	2.50
A_{44}	1.00	1.0084	1.00	1.000	3.50	11.00	3.50	3.50	2.50
A_{45}	7.50	7.5103	7.50	7.239	7.00	11.00	3.50	11.00	12.00
A_{46}	4.50	5.2449	6.50	4.424	2.50	11.00	3.50	3.50	5.00
A_{47}	1.00	1.0550	1.00	1.001	21.00	11.00	3.50	3.50	5.00
				Final dome configuration					
nsm	30	30	30	30	24	24	24	26	24
nnp	390	390	390	390	312	312	312	338	312
nbar	1410	1410	1410	1410	1128	1128	1128	1222	1128
				Objective functions and constraints					
W (kg)	10558	10504	11045	10101.36	10949	16482	10836	10066	9507
f_1 (Hz)	7.0004	7.002	7.0008	7.002	7.0002	8.9266	7.0511	7.0674	7.2536
f_3 (Hz)	9.0055	9.001	9.0068	9.002	9.0001	9.1078	9.0057	9.0001	9.0420
nfe	18000	20000	20000	10000	30000	6000	9000	12000	15000

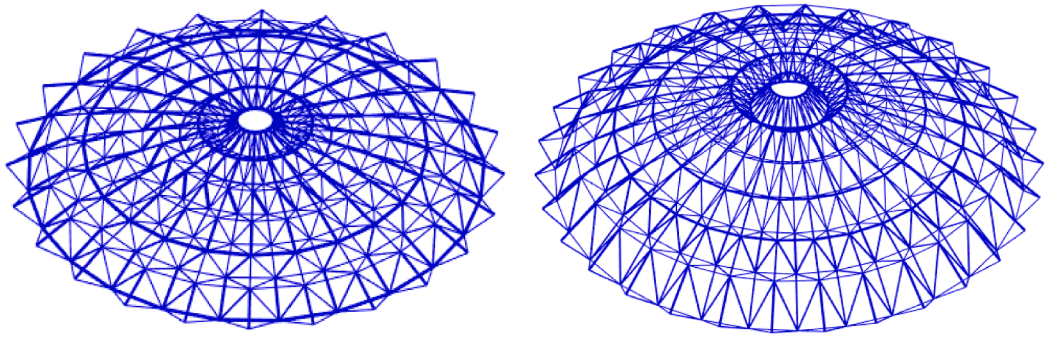

(a) Case #1 – 10949 kg (b) Case #2 – 10558 kg

Fig. 15. The best configurations of the 1410-bar double-layer truss dome when cardinality constraints are not considered. The different thicknesses, not to scale, represent the different cross-sectional areas of each one of the bars.

the sizing design variables were present in the optimization problem. See Fig. 7.

6.2. A 600-bar single-layer truss dome

This dome was analyzed by Kaveh et al. [68], Carvalho et al. [30], and Kaveh and Javadi [56]. A standard module was detailed in [68,56] to provide the mesh generation of the complete dome. This module is given again in Fig. 8, alongside one possible consecutive neighbor module. An example of a complete dome with thirty modules is depicted in Fig. 9. The original dome presents twenty-four standard modules.

The dome is 13 m in diameter and 7.5 m in height. Each bar of this substructure is considered a sizing design variable, leading to an optimization problem with twenty-five variables. The elastic modulus is 200 GPa, the material density is 7850 kg/m^3, and the nodes at the bottom of the dome (coordinates $Z = 0$) are completely restricted. A nonstructural mass of 100 kg is added at all free nodes. The discrete search space for this problem is defined in the range $1.0, 1.5, 2.0, 2.5, 3.0, \ldots, 99.0, 99.5,$ and 100 cm^2. The bounds for the natural frequencies of vibration are $f_1 \geqslant 5$ Hz and $f_3 \geqslant 7$ Hz, and the number of standard modules must be in the range $18 \leqslant nsm \leqslant 30$.

Three cases (#1, #2 and #3) are analyzed in this experiment, where *ndv* means the number of design variables in the following descriptions:

- In Case #1, only the sizing design variables (cross-sectional areas of the bars) are set ($ndv = 25$).
- In Case #2, a layout design variable (number of standard modules or *nsm*) is added ($ndv = 26$).
- Case #3 considers sizing (cross-sectional areas of the bars), layout design variables (number of standard modules or *nsm*), and a cardinality constraint m setting the maximum number of distinct cross-sectional areas of the bars ($ndv = 26 + m$).

Table 3 shows the results for Cases #1 to #3 of the 600-bar truss dome. The results provided in columns 3, 4, and 5 are from Kaveh et al. [68], Carvalho et al. [30], and Kaveh and Javadi [56], respectively. These results will be compared with the result presented in column 1. Enhanced colliding bodies optimization is employed, with a cascade optimization procedure that is used in [68], a craziness based particle swarm optimization (CRPSO) as the search algorithm adopted in [30], and a chaos-based firefly algorithm in [56].

Fig. 10 shows the best results for the 600-bar truss dome for Cases #1 and #2, respectively. Fig. 11 shows the best configurations for the 600-bar truss dome when the cardinality constraints are considered (Case #3). The different colors indicate the different cross-sectional areas adopted in each group in the optimized solutions.

The best results of the 600-bar single-layer truss dome are shown in Table 3. Case #1 of this experiment found a final weight equal to 6196 kg against 6175 kg, 6132 kg, and 6058.49 kg found in [68,30,56],

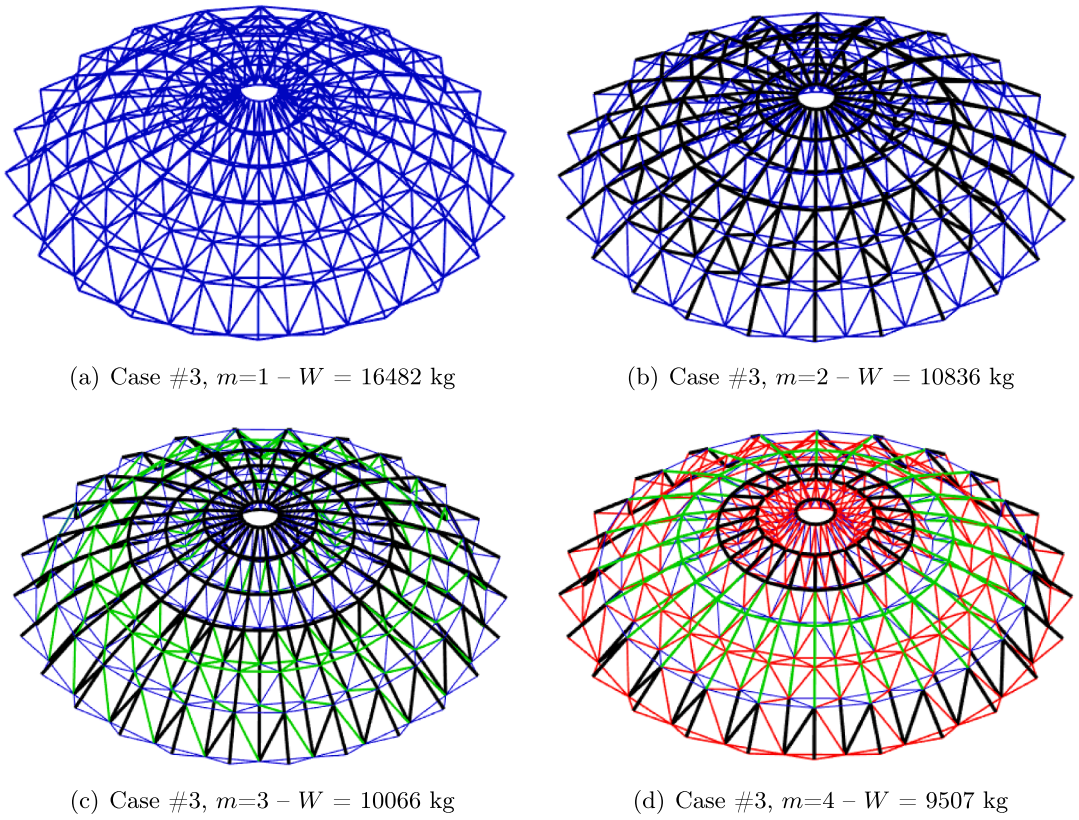

(a) Case #3, m=1 – W = 16482 kg (b) Case #3, m=2 – W = 10836 kg

(c) Case #3, m=3 – W = 10066 kg (d) Case #3, m=4 – W = 9507 kg

Fig. 16. The best configurations of the 1410-bar double-layer truss dome when cardinality constraints are considered. The different colors indicate the different cross-sectional areas adopted in each group in the optimized solutions.

respectively. The final weight is 2.27% heavier than the best solution in this comparison. The result can be considered very competitive in this comparison. It is important to remark that only the sizing design variables are considered.

Adding a layout design variable (Case #2), the final weight is equal to 5957 kg, with 19 standard modules, 171 nodes, and 475 bars, against 6196 kg, with 24 standard modules, 216 nodes, and 600 bars in the original configuration of this dome. There is a gain of 3.85% in this optimized solution. Also, the number of bars was reduced from 600 to 475 (79.16% of the original configuration). Finally, a desirable aspect is the number of nodes, 171 versus 216, indicating that 79.19% of the initial structural configuration directly impacts the number of connections to be fabricated and installed.

For Case #3, setting cardinality constraints, the results for the 600-bar single-layer truss dome are encouraging and very interesting. Except for $m = 1$ (6947 kg), the results for $m = 2$ (5776 kg), $m = 3$ (5360 kg), and $m = 4$ (5282 kg) are very good. Especially note the result for $m = 4$, where using only four distinct cross-sectional areas, the final weight (5282 kg) is better than all the solutions obtained without cardinality constraints, leading to a real gain in the optimized structure. Furthermore, this result is better than those presented in [68,30,56], providing counter-intuitive solutions concerning a new member grouping of bars as well as the number of standard modules. All the constraints are satisfied, and the optimized solutions are rigorously feasible. In all the experiments, the constraint regarding the second natural frequency of vibration was active. Also, in four of these experiments, the two constraints were active. The trade-off between weight and number of different cross-sectional areas for the 600-bar single-layer truss dome is provided in Fig. 12.

Fig. 6.2 depicts the trade-off between the weights and the numbers of different cross-sectional areas for the 600-bar truss dome for all cases. Note that the weights decrease as the number of distinct cross-sectional areas increases, as expected.

6.3. A 1410-bar double-layer truss dome

The 1410-bar double-layer truss dome is shown in Fig. 13, as presented by Kaveh et al. [68]. Again, the standard module of this structure is given in Fig. 14 alongside one possible consecutive neighbor module. The structure is composed of 30 standard modules, 390 nodes, and 1410 elements, as shown in Fig. 13. The dome is 13 m in diameter and 4.5 m in height. The total number of sizing design variables is forty-seven. The elastic modulus is 200 GPa, and the material density is 7850 kg/m^3. A nonstructural mass of 100 kg is attached to all the free nodes, and the discrete search space is defined by the following cross-sectional areas: $1.0, 2.0, 3.0, 4.9, 5.0 \ldots 98.0, 99.0,$ and 100 cm^2. The limits for the natural frequencies are $f_1 \geqslant 7$ Hz and $f_3 \geqslant 9$ Hz, and the number of standard modules must be in the range $24 \leqslant nsm \leqslant 36$. As in the 600-bar truss dome, the same three cases are analyzed in this experiment, and the number of design variables ndv, are 47, 48, and 48 + m, for Cases #1, #2, and #3, respectively.

Tables 4 and 5 shows the results for Cases #1 to #3 of the 1410-bar double-layer truss dome. The results are provided in columns 3, 4, and 5 from [68,30,56], respectively. These results will be compared with the result presented in column 1.

Fig. 15 shows the best results for the 1410-bar double-layer truss dome for Cases #1 and #2, respectively. Fig. 16 shows the best configurations for the 1410-bar truss dome when the cardinality constraints are considered (Case #3). The different colors indicate the different cross-sectional areas adopted in each group in the optimized solutions.

From the results provided in Table 5, one can observe that the final weight found for Case #1 of the 1410-bar double-layer dome was equal to 10558 kg against 10504 kg, 11045, kg and 10101.36 kg presented by Kaveh et al. [68], Carvalho et al. [30], and Kaveh and Javadi [56],

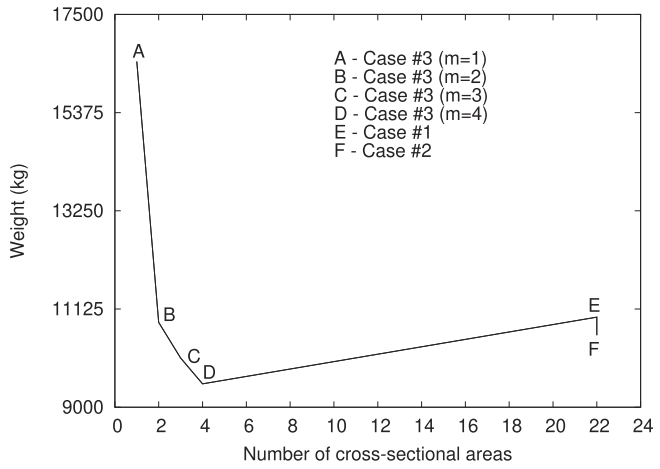

Fig. 17. The trade-off between weight and number of different cross-sectional areas for the 1410-bar double-layer truss dome.

respectively. The final weight is 4.52% heavier than the best solution in this comparison considering only the sizing design variables.

The results for the 1410-bar double-layer dome provided in Table 5 show that when the number of standard modules is considered as a layout design variable (Case #2), the optimized structure has twenty-four modules versus thirty modules present in the original configuration. The number of bars is reduced from 1410 to 1128 and the number of nodes from 390 to 312, and the final weight obtained is equal to 10949 kg. This weight is 4.24% higher than the solution obtained by Kaveh et al. [68], which was 10504 kg, and 8.39% by Kaveh and Javadi [56], which was 10101.36 kg. However, the numbers of nodes and bars were reduced to 80% of the original configuration, leading to real gains in the fabrication, assembling, checking, foundation elements, etc. of the optimized dome obtained in this proposed experiment.

For Case #3, the results obtained are even more interesting. One can observe that for $m = 4$, the final best weight is equal to 9507 kg (90% of the final weight obtained by Kaveh et al. [68], equal to 10504 kg, and assigning for the bars only four distinct cross-sectional areas). Also, the number of standard modules is reduced from 30 to 24 and the number of nodes from 390 to 312. In the same way, the final weight, reached with $m = 3$, is extremely interesting and competitive. This solution has a final weight equal to 10066 kg, which is better than those found in this study with no cardinality constraint and no layout design variable, 10558 kg, 10504 kg (Cases #1 and #2), and 11045 kg, obtained by Kaveh et al. [68] and Carvalho et al. [30].

It is easy to observe that setting $m = 4$ with the new layout design variable is much better than using the original optimization problem formulation. All the constraints are satisfied, and the optimized solutions are rigorously feasible. In six experiments, the constraint regarding the first and second natural frequencies of vibration were active. In six of the eight experiments, the two constraints imposed on the optimization problem are active. The trade-off between weight and number of different cross-sectional areas for the 1410-bar double-layer truss dome is provided in Fig. 17.

Fig. 6.3 depicts the trade-off between the weights and the numbers of different cross-sectional areas for the 1410-bar truss dome for all cases. Note that the weights decrease as the number of distinct cross-sectional areas increases, as expected.

Table 6
Statistical results and computational times for the second set of numerical experiments.

Case #	Best	Median	Average	Std	Worst	nfr	Time (s)
120-bar single-layer truss dome							
1	10310	10311	10310	0.41	10312	20	88
2	8375	8387	8388	5.67	8392	20	38
$3m = 1$	3780	3821	3794	75.26	4116	20	62
$3m = 2$	2244	2471	2329	261.13	3249	20	47
$3m = 3$	2122	2404	2378	214.01	2847	20	39
$3m = 4$	1995	2380	2410	184.91	2668	20	48
600-bar single-layer truss dome							
1	5957	8209	9309	2006	14758	20	1504
2	6196	8580	7555	1046	9896	20	5692
$3m = 1$	6947	7381	7306	724	9552	20	572
$3m = 2$	5776	6787	6676	403	7769	20	850
$3m = 3$	5360	5925	6045	411	6796	20	1134
$3m = 4$	5252	6259	6039	485	6922	20	1402
1410-bar double-layer truss dome							
1	10949	14508	16408	2797	23506	20	28572
2	10558	10694	10729	70	10919	20	10888
$3m = 1$	16482	16482	16725	519	18132	20	5420
$3m = 2$	10836	12560	13356	1470	16041	20	7987
$3m = 3$	10066	12213	11893	1406	14626	20	11201
$3m = 4$	9507	10083	11237	1186	13845	20	14101

6.4. Statistical results

Table 6 presents the statistical results and computational times for the numerical experiments, where *Std* means the standard deviation and *nfr* means the number of runs that achieved a feasible solution. The computer processor was an Intel i5 7600 k, with 16 GB of RAM, and Matlab® was the main language used in which the optimization algorithm was encoded, with a simulator in C language for the structural analysis.

7. Conclusions and future work

The optimization algorithms simultaneously considered sizing, shape, and layout design variables to find the minimization of the mass as well as the task of finding the best member grouping automatically. To obtain automatic variable linking to search for the best member grouping of the bars of the domes analyzed in this paper, a special encoding involving cardinality constraints is considered.

Previous studies [34,69,30] show that the advantages of discovering new member grouping can lead to economy in fabrication, checking, transportation, and so on, using a reduced number of distinct cross-sectional areas. For example, reducing the fabrication costs when setting them in the machine to laminate a few items can accelerate production costs, leading to savings in the final costs of the profiles. Also, labor savings are reached when the structure is welded, checked, etc.

New structural optimization problems are analyzed in this paper, which presents interesting counter-intuitive results. Trade-off curves show the optimized weights in comparison with the number of distinct cross-sectional areas used in the solutions. These curves also show that the consideration of layout design variables and the optimal grouping of the bars, setting cardinality constraints, significantly improve the results compared to the cases where only the sizing design variables were present in the optimization problem.

Comparative studies showed that the results obtained were better than those presented in the literature. These results are expected to be used for comparisons in future works.

The main objective of this paper is on the applications strategies and optimization algorithms, respectively, in finding solutions of simultaneous sizing, shape, and layout optimization of dome structures. Sometimes, these problems are difficult to handle using traditional methods.

The results show that for the traditional problems found in the literature (the second and third numerical experiments), the optimal solutions can be considered competitive and innovative, where the layout design variable can lead to the discovery of counter intuitive

solutions.

Future works will consider, in the same optimization problems, static loads, self-weight loads, and those arising from the environment, such as wind and earthquake dynamic actions. Topology optimization problems considering the best member grouping and the best material combination presenting nonlinear behavior are attractive points to be investigated in future works.

It is possible to formulate and investigate a new optimization problem using a more sophisticated fitness function. It may reflect the total costs associated with aspects related to fabrication, transportation, storing, checking, connections, foundations elements, and so on. Extensions of this paper will consider other structures, such as planes and spatial frames. Additionally, the multi-objective optimization will be formulated (e.g. minimizing the weight and maximizing the first natural frequency of vibration and the load factor concerning the global stability).

Declaration of Competing Interest

The authors declare that they have no known competing financial interests or personal relationships that could have appeared to influence the work reported in this paper.

Acknowledgments

This study was financed in part by the Coordenação de Aperfeiçoamento de Pessoal de Nível Superior in Brasil (CAPES), Finance Code 001, and the Conselho Nacional de Desenvolvimento Científico e Tecnológigo (CNPq), Grant 306186/2017. The authors would like to thanks the reviewers for the corrections and suggestions, which helped improve the quality of the paper.

References

[1] Barbosa HJC, Lemonge ACC. A genetic algorithm encoding for a class of cardinality constraints. In: Proceedings of the 7th annual conference on Genetic and evolutionary computation. ACM Press; 2005. p. 1193–200.
[2] Storn R, Price K. Differential evolution a simple and efficient adaptive scheme for global optimization over continuous spaces. Tech. Rep. 95-012, Univ. of California, Berkeley, CA; 1995.
[3] Barbosa HJC. Lemonge ACC. An adaptive penalty scheme in genetic algorithms for constrained optimization problems. In GECCO'02: Proceedings of the genetic and evolutionary computation conference, New York, 9–13 July 2002. Morgan Kaufmann Publishers. p. 287–94.
[4] Lemonge ACC, Barbosa HJC. An adaptive penalty scheme for genetic algorithms in structural optimization. Int J Numer Methods Eng 2004;59(5):703–36.
[5] Bendsøe MP, Sigmund O. Topology optimization: theory, methods, and applications. Springer Science & Business Media; 2013.
[6] Mela K. Resolving issues with member buckling in truss topology optimization using a mixed variable approach. Struct Multidiscip Optim 2014;50(6):1037–49.
[7] Ramos AS, Paulino GH. Convex topology optimization for hyperelastic trusses based on the ground-structure approach. Struct Multidiscip Opt 2015;51(2): 287–304.
[8] Kanno Y. Global optimization of trusses with constraints on number of different cross-sections: a mixed-integer second-order cone programming approach. Comput Optim Appl 2016;63(1):203–36.
[9] Zhang XS, Paulino GH, Ramos AS. Multi-material topology optimization with multiple volume constraints: a general approach applied to ground structures with material nonlinearity. Struct Multidiscip Optim 2018;57(1):161–82.
[10] Ohsaki M. Genetic algorithm for topology optimization of trusses. Comput Struct 1995;57(2):219–25.
[11] Hajela P, Lee E. Genetic algorithms in truss topological optimization. Int J Solids Struct 1994;32:3341–57.
[12] Rajan SD. Sizing, shape, and topology design optimization of trusses using genetic algorithm. J Struct Eng 1995;121:1480–7.
[13] Tang W, Tong L, Gu Y. Improved genetic algorithm for design optimization of truss structures with sizing, shape and topology variables. Int J Numer Meth Eng 2005; 62(13):1737–62.
[14] Giger M, Ermanni P. Evolutionary truss topology optimization using a graph-based parameterization concept. Struct Multidiscip Optim 2006;32(4):313–26.
[15] Rahami H, Kaveh A, Gholipour Y. Sizing, geometry and topology optimization of trusses via force method and genetic algorithm. Eng Struct 2008;30(9):2360–9.
[16] Chen S-Y, Shui X-F, Huang H. Improved genetic algorithm with two-level approximation using shape sensitivities for truss layout optimization. Struct Multidiscip Optim 2017;55(4):1365–82.
[17] Assimi H, Jamali A, Nariman-zadeh N. Sizing and topology optimization of truss structures using genetic programming. Swarm Evol Comput 2017;37:90–103.
[18] Miguel LFF, Lopez RH, Miguel LFF. Multimodal size, shape, and topology optimisation of truss structures using the firefly algorithm. Adv Eng Softw 2013;56: 23–37.
[19] Wu Y, LIi Q, Hu Q, Borgart A. Size and topology optimization for trusses with discrete design variables by improved firefly algorithm. Math Prob Eng 2017;2017: 1–13.
[20] Luh G-C, Lin C-Y. Optimal design of truss-structures using particle swarm optimization. Comput Struct 2011;89:2221–32.
[21] Mortazavi A, Toğan V. Simultaneous size, shape, and topology optimization of truss structures using integrated particle swarm optimizer. Struct Multidiscip Optim 2016;54(4):715–36.
[22] Wu C-Y, Tseng K-Y. Truss structure optimization using adaptive multi-population differential evolution. Struct Multidiscip Optim 2010;42(4):575–90.
[23] Huang X, Xie YM. Convergent and mesh-independent solutions for the bi-directional evolutionary structural optimization method. Finite Elem Anal Des 2007;43(14):1039–49.
[24] Zuo ZH, Xie YM. A simple and compact python code for complex 3d topology optimization. Adv Eng Softw 2015:1–11.
[25] Kitayama S, Arakawa M, Yamazaki K. Differential evolution as the global optimization technique and its application to structural optimization. Appl Soft Comput 2011;11(4):3792–803.
[26] Ahrari A, Atai A, Deb K. Simultaneous topology, shape and size optimization of truss structures by fully stressed design based on evolution strategy. Eng Optim 2015;47(8):1063–84.
[27] Ho-Huu V, Nguyen-Thoi T, Nguyen-Thoi MH, Le-Anh L. An improved constrained differential evolution using discrete variables (d-icde) for layout optimization of truss structures. Exp Syst Appl 2015;42(20):7057–69.
[28] Kaveh A, Mahdavi VR. Colliding bodies optimization for size and topology optimization of truss structures. Struct Eng Mech 2015;53(5):847–65.
[29] Savsani VJ, Tejani GG, Patel VK, Savsani P. Modified meta-heuristics using random mutation for truss topology optimization with static and dynamic constraints. J Comput Des Eng 2017;4(2):106–30.
[30] Carvalho JPG, Lemonge ACC, Carvalho ECR, Hallak PH, Bernardino HS. Truss optimization with multiple frequency constraints and automatic member grouping. Struct Multidiscip Optim 2018;57(2):547–77.
[31] Grierson DE, Cameron GE. Soda-structural optimization design and analysis. Waterloo, Ontario, Canada: Waterloo Engineering Software; 1987.
[32] Galante M. Genetic algorithms as an approach to optimize real-world trusses. Int J Numer Methods Eng 1996;39(3):361–82.
[33] Fenves ST, Shea K, Cagan J. A shape annealing approach to optimal truss design with dynamic grouping of members. J Mech Des 1997;119(3):388–94.
[34] Barbosa HJC, Lemonge ACC, Borges CCH. A genetic algorithm encoding for cardinality constraints and automatic variable linking in structural optimization. Eng Struct 2008;30:3708–23.
[35] Lemonge ACC, Barbosa HJC, da Fonseca LG, Coutinho ALGA. A genetic algorithm for topology optimization of dome structures. In: Proceedings of the 2nd international conference on engineering optimization – EngOpt, Lisbon, Portugal; 2010.
[36] Lemonge ACC, Barbosa HJC, Coutinho ALGA, Borges CCH. Multiple cardinality constraints and automatic member grouping in the optimal design of steel framed structures. Eng Struct 2011;33(2):433–44.
[37] Kaveh A, Zolghadr A. A multi-set charged system search for truss optimization with variables of different natures; element grouping. Periodica Polytechnica. Civil Eng 2011;55(2):87.
[38] Herencia JE, Haftka RT, Balabanov V. Structural optimization of composite structures with limited number of element properties. Struct Multidiscip Optim 2013;47(2):233–45.
[39] Guo HY, Li ZL. Structural topology optimization of high-voltage transmission tower with discrete variables. Struct Multidiscip Optim 2011;43(6):851–61.
[40] Liu X, Cheng G, Wang B, Lin S. Optimum design of pile foundation by automatic grouping genetic algorithms. ISRN. Civil Eng 2012;2012.
[41] Liu X, Cheng G, Yan J, Jiang L. Singular optimum topology of skeletal structures with frequency constraints by AGGA. Struct Multidiscip Optim 2012;45(3):451–66.
[42] Kripka M, Medeiros GF, Lemonge ACC. Use of optimization for automatic grouping of beam cross-section dimensions in reinforced concrete building structures. Eng Struct 2015;99:311–8.
[43] Souza RR, Miguel LFF, Lopez RH, Miguel LFF, Torii AJ. A procedure for the size, shape and topology optimization of transmission line tower structures. Eng Struct 2016;111:162–84.
[44] Tugilimana A, Coelhoand RF, Thrall AP. An integrated design methodology for modular trusses including dynamic grouping, module spatial orientation, and topology optimization. Struct Multidiscip Optim 2019:p. 1–26.
[45] Kaveh A, Izadifard RA, Mottaghi L. Cost optimization of rc frames using automated member grouping. Iran University of Science & Technology 2020;10(1):91–100.
[46] Saka MP, Ulker M. Optimum design of geometrically nonlinear space trusses. Comput Struct 1992;42(3):289–99.
[47] Ebenau Carsten, Rottschäfer Jens, Thierauf Georg. An advanced evolutionary strategy with an adaptive penalty function for mixed-discrete structural optimisation. Adv Eng Softw 2005;36(1):29–38.
[48] Saka MP. Optimum topological design of geometrically nonlinear single layer latticed domes using coupled genetic algorithm. Comput Struct 2007;85(21–22): 1635–46.
[49] Kameshki ES, Saka MP. Optimum geometry design of nonlinear braced domes using genetic algorithm. Comput Struct 2007;85(1–2):71–9.

[50] Kaveh A, Talatahari S. Optimal design of single layer domes using meta-heuristic algorithms; a comparative study. Int J Space Struct 2010;25(4):217–27.
[51] Kaveh Ali, Talatahari Siamak. Geometry and topology optimization of geodesic domes using charged system search. Struct Multidiscip Optim 2011;43(2):215–29.
[52] Çarbaş Serdar, Saka Mehmet P. Optimum topology design of various geometrically nonlinear latticed domes using improved harmony search method. Struct Multidiscip Optim 2012;45(3):377–99.
[53] Babaei M, Sheidaii MR. Automated optimal design of double-layer latticed domes using particle swarm optimization. Struct Multidiscip Optim 2014;50(2):221–35.
[54] Saeid Kazemzadeh Azad. Enhanced hybrid metaheuristic algorithms for optimal sizing of steel truss structures with numerous discrete variables. Struct Multidiscip Optim 2017;55(6):2159–80.
[55] Ji-Yang Fu, Ben-Gang Wu, Jiu-Rong Wu, Deng Ting, Pi Yong-Lin, Xie Zhuang-Ning. Design sensitivity analysis for optimal design of geometrically nonlinear lattice structures. Eng Struct 2018;168:915–28.
[56] Kaveh A, Javadi SM. Chaos-based firefly algorithms for optimization of cyclically large-size braced steel domes with multiple frequency constraints. Comput Struct 2019;214:28–39.
[57] Mortazavi Ali. Interactive fuzzy search algorithm: A new self-adaptive hybrid optimization algorithm. Eng Appl Artif Intell 2019;81:270–82.
[58] Mortazavi Ali. Size and layout optimization of truss structures with dynamic constraints using the interactive fuzzy search algorithm. Eng Optim 2020:1–23.
[59] Bathe KJ. Finite element procedures. Pearson Education Inc: Prentice Hall; 2006.
[60] McGuire W, Gallagher RH, Ziemian RD. Matrix structural analysis. 2nd ed. New York: John Wiley & Sons; 2014.
[61] Kukkonen S, Lampinen J. GDE3: The third evolution step of generalized differential evolution. In Evolutionary Computation, 2005. The 2005 IEEE Congress on, vol. 1, IEEE; 2005. p. 443–450.
[62] Vargas DEC, Lemonge ACC, Barbosa HJC, Bernardino HS. Differential evolution with the adaptive penalty method for structural multi-objective optimization. Optim Eng 2019;20(1):65–88.
[63] Price K, Storn RM, Lampinen JA. Differential evolution: a practical approach to global optimization. Springer Science & Business Media; 2006.
[64] Boscardin JT, Yepes V, Kripka M. Optimization of reinforced concrete building frames with automated grouping of columns. Autom Constr 2019;104:331–40.
[65] Krempser Eduardo, Bernardino Heder S, Barbosa Helio JC, Lemonge Afonso CC. Performance evaluation of local surrogate models in differential evolution-based optimum design of truss structures. Eng Comput 2017.
[66] Saka MP, Ulker M. Optimum design of geometrically non-linear space trusses. Comput Struct 1991;41:1387–96.
[67] Ebenau C, Rotsschafer J, Thierauf G. An advanced evolutionary strategy with an adaptive penalty function for mixed-discrete structural optimisation. Adv Eng Softw 2005;36:29–38.
[68] Kaveh A, Ilchi Ghazaan M. Optimal design of dome truss structures with dynamic frequency constraints. Struct Multidiscip Optim 2016;53(3):605–21.
[69] Lemonge ACC, Barbosa HJC, Coutinho ALGA, Borges CCH. Multiple cardinality constraints and automatic member grouping in the optimal design of steel framed structures. Eng Struct 2011;33:433–44.